Journal of Electroanalytical Chemistry 880 (2021) 114834

Contents lists available at ScienceDirect

Journal of Electroanalytical Chemistry

journal homepage: www.elsevier.com/locate/jelechem

P2-type layered structure $Na_{1.0}Li_{0.2}Mn_{0.7}Ti_{0.1}O_2$ as a superb electrochemical performance cathode material for sodium-ion batteries

Nguyen V. To [a], Ky V. Nguyen [a], Hieu S. Nguyen [b], Son T. Luong [a], Phat T. Doan [a], Thu Hoa T. Nguyen [d], Quyen Q. Ngo [a,*], Nghia V. Nguyen [c,d,**]

[a] Department of Chemical Physics, Le Qui Don Technical University, 236 Hoang Quoc Viet, Cau Giay, Hanoi, 100000, Viet Nam
[b] Institute of Materials Science, VAST, 18 Hoang Quoc Viet, Hanoi, 100000, Viet Nam
[c] Research Center of Advanced Materials and Applications, Institute of Architecture, Construction, Urban, and Technology, Hanoi Architectural University, Hanoi, 100000, Viet Nam
[d] Department of Physics, Open Training Institute, Hanoi Architectural University, Hanoi, 100000, Viet Nam

ARTICLE INFO

Article history:
Received 26 June 2020
Received in revised form 1 November 2020
Accepted 5 November 2020
Available online 10 November 2020

Keywords:
Sodium ion battery
P2-type layered structure material
$Na_{1.0}Li_{0.2}Mn_{0.7}Ti_{0.1}O_2$
High specific capacity
Excellent rate capacity

ABSTRACT

P2-type layered structure manganese-based materials have been reported as the most promising candidates for practical applications of sodium ion batteries because of their high capacity, facile fabrication, low cost, and environmental friendliness. In this work, a new P2-type layered structure $Na_{1.0}Li_{0.2}Mn_{0.7}Ti_{0.1}O_2$ material was successfully synthesized by a conventional solid-state reaction method. The material delivered a superior specific capacity of 163 mAh g^1 at 0.1C within the potential range from 1.5 to 4 V. The capacity and the coulombic efficiency of the material remained of 90% and 97% after 50 cycles of charge/discharge at a rate of 0.1C. The material also exhibited an excellent rate capability, with a discharge capacity of over 100 mAh.g^{-1} remained at a rate of 1.0C. The observed results suggested that $Na_{1.0}Li_{0.2}Mn_{0.7}Ti_{0.1}O_2$ is a promising cathode material for sodium ion batteries.

1. Introduction

Recently, scientists have intensively investigated the characteristics of cathode materials that are suitable for practical applications of sodium ion batteries (SIBs). Numerous P2-type layered-structure materials have been reported for SIBs due to their high energy density compared to the others [1–9]. Among the P2-structure materials, solely manganese-based oxides have a moderated electrochemical performance, especially the high cycling ability. Caballero et al. reported that P2-$Na_{0.66}MnO_2$ cell had a capacity of 160 mAh g^{-1}, which rapidly decreased to 60 mAh g^{-1} after 10 cycles [10]. P2-$Na_{0.7}MnO_{2+z}$ material showed the similar characteristics in which the capacity of the material was 140 mAh g^{-1} and remained at 70 mAh g^{-1} after 20 cycles [11]. P2-type $Na_{0.53}MnO_2$ exhibited a discharge capacity of 120 mAh g^{-1} at 0.2C, and the capacity reduced to about 90 mAh g^{-1} after 50 cycles [5].

Mixing manganese with other transition metals has improved the cycling ability and rate capability of the manganese-based oxide [1,6,12–14]. P2-type $Na_x[Fe_{1/2}Mn_{1/2}]O_2$ delivered a capacity of 190 mAh g^{-1} at a rate of 12 mA g^{-1} between 1.5 and 4.3 V, and the capacity remained at 150 mAh g^{-1} after 30 cycles [13]. P2-$Na_{2/3}Ni_{1/3}Mn_{2/3}O_2$ exhibited a capacity of 150 mAh g^{-1} at 10 mA g^{-1} between 2.0 and 4.5 V, with a remaining capacity of 70% after 30 cycles [8]. Pang et al. reported that doping of Co and Cu generated a synergetic improvement of multi-metallic ions which improved electrode kinetics of P2-type $Na_{2/3}Mn_{1/2}Co_{1/3}Cu_{1/6}O_2$ oxide [6]. The material had a capacity of 118.2 mAh g^{-1} at a current density of 10 mA g^{-1} and retained 66% of its capacity after 100 cycles. Similar synergetic improvement of multi-metallic ions reported by Zhao et al. who showed that over 90% of capacity of P2-$Na_{2/3}Ni_{2/9}M_{1/9}Mn_{2/3}O_2$ (M = Mg, Al, Fe, Co) could have remained after 30 cycles [14].

It has been reported that substitution of a small amount of lithium stabilized the structure of manganese-based oxides. $Na_{0.6}Li_{0.2}Mn_{0.8}O_2$ with a P2 structure exhibited an initial discharge capacity of 247 mAh g^{-1} for lithium-ion batteries and a stable capacity over 240 mAh g^{-1} after 30 cycles [15]. Our previous work showed that P2-$NaLi_{0.2}Mn_{0.8}O_2$, as a cathode material for SIBs, delivered a capacity of 241 mAh g^{-1} and a capacity retention of 78% after 40 cycles [16]. Kim et al., reported that P2-type

* Corresponding author at: Department of Chemical Physics, Le Qui Don Technical University, 236 Hoang Quoc Viet, Cau Giay, Hanoi, 100000, Viet Nam.
** Corresponding author at: Research Center of Advanced Materials and Applications, Institute of Architecture, Construction, Urban, and Technology, Hanoi Architectural University, Hanoi, 100000, Viet Nam.
E-mail addresses: quyenkazan@gmail.com (Q.Q. Ngo), nghianv@hau.edu.vn (N.V. Nguyen).

http://dx.doi.org/10.1016/j.jelechem.2020.114834

$Na_{1.0}Li_{0.2}Mn_{0.75}Ni_{0.25}O_{2.35}$ material had a capacity of 114 mAh g^{-1} and the capacity retention was about 98% after 50 cycles [17]. Titanium substituted $Na_{2/3}Ni_{1/4}Ti_xMn_{3/4-x}O_2$ cathode material delivered a reversible capacity of 140 mAh g^{-1}, which was remained over 92% after 25 cycles [18]. The better cyclability and rate capability of $Na_{2/3}Ni_{1/4}Ti_xMn_{3/4-x}O_2$ compared to the pristine P2-$Na_{2/3}Ni_{1/4}Mn_{3/4}O_2$ were attributed to the P2-structure stabilization of Ti substitution. Ti-substituted $Na_{0.44}[Mn_{1-x}Ti_x]O_2$ with tunnel structure showed a capacity of 110 mAh g^{-1} and a capacity retention of over 96% after 1100 cycles [19] . P2-$Na_{0.66}[Cr_{0.6}Ti_{0.4}]O_2$ exhibited a capacity of 75 mAh g^{-1} at 0.1C between 2.5 and 3.85 V and the capacity was stable over 200 cycles [9] . Thus, we believed that the substitution of titanium may results in an enhancement of the electrochemical performance of the P2-type layered structure cathode materials.

In this work, a P2-type layered structure $Na_{1.0}Li_{0.2}Mn_{0.7}Ti_{0.1}O_2$ material was successfully synthesized by a conventional solid-state reaction method. Lithium and titanium were chosen to substitute for manganese for the purpose of retaining the high capacity and enhancing the cycling ability and rate capability of the sodium-manganese-based material. The electrochemical performances of the $Na_{1.0}Li_{0.2}Mn_{0.7}Ti_{0.1}O_2$ material for sodium-ion batteries were investigated in detail. The results revealed that the $Na_{1.0}Li_{0.2}Mn_{0.7}Ti_{0.1}O_2$ material had a superior capacity, good cycling ability, and high rate capability.

2. Experimental

2.1. Synthesis of micro plate-like shape $Na_{1.0}Li_{0.2}Mn_{0.7}Ti_{0.1}O_2$ material

Micro plate-like shape $Na_{1.0}Li_{0.2}Mn_{0.7}Ti_{0.1}O_2$ material was synthesized by a conventional solid-state reaction method. Stoichiometric amounts of Na_2CO_3 (Sigma-Aldrich, 99.5%), Li_2CO_3 (Sigma-Aldrich, 99.0%), $MnCO_3$ (Sigma-Aldrich, ≥ 99.9%), and TiO2 (Sigma-Aldrich, 99.9%) were mixed and carefully ground using a mortar and pestle. The mixture was heated at 500 °C for 10 h in the air and naturally cooled down to room temperature to remove the carbonate. The powder then was ground again, calcined at 730 °C for 20 hoursh in the air and quenched to room temperature to obtain the $Na_{1.0}Li_{0.2}Mn_{0.7}Ti_{0.1}O_2$ material. The material was reserved in a glove box to avoid moisture adsorption. The expected reaction to form the $Na_{1.0}Li_{0.2}Mn_{0.7}Ti_{0.1}O_2$ oxide was:

$$5Na_2CO_3 + Li_2CO_3 + 7MnCO_3 + TiO_2 + 2.5O_2 \rightarrow 10Na_{1.0}Li_{0.2}Mn_{0.7}Ti_{0.1}O_2 + 13CO_2$$

2.2. Material characterizations

The crystal structure of the $Na_{1.0}Li_{0.2}Mn_{0.7}Ti_{0.2}$ material was identified by X-ray diffraction (XRD, Bruker D8 Advance, Cu Kα radiation, λ = 1.5406 Å). The XRD data were collected in the diffraction angle range (2θ) between 10° and 70° at a step of 0.03° per second. The morphology of the material was observed using scanning electron microscopy (SEM, JEOL, JSM-6490) and transmission electron microscopy (TEM, Hitachi-H7100). The adsorption and desorption isotherms were measured using N_2 gas at 77 K by a Tristar 3000 Micromeritics instrument. The BET surface area was calculated using adsorption data in a relative pressure range of 0.05–0.25.

2.3. Electrochemical measurements

The $Na_{1.0}Li_{0.2}Mn_{0.7}Ti_{0.2}$ material (80 wt%), super P carbon black (10 wt%) (Alfa Aesar, 99 + %), and polyvinylidene fluoride (10 wt%) (PVDF, Alfa Aesar) were added into *N*-methyl-2-pyrrolidone (Alfa Aesar, 99 + %) solvent and ball milled to form a homogeneous slurry. The slurry was coated onto a 15 μm-thick Al foil current collector and dried at 100 °C for 12 h in a vacuum oven. The resulted tape was rolling pressed to increase the density and cut into 16 mm diameter circles for using as the positive electrode. The negative electrode was pure sodium foil (Acros Organic). The electrolyte solution contained 1 M sodiumperchlorate ($NaClO_4$) in ethylene carbonate (EC) and diethylene carbonate (DEC) (1,1 by volume). The separator was polypropylene (PP, TOB New Energy). Electrochemical tests were conducted using 2032 coin-type cells. The coin cells were assembled in a glove box with oxygen and moisture level less than 0.1 ppm and stabilized for 12 h before testing. The charge/discharge measurements were taken on a NEWARE battery tester. The cyclic voltammetry (CV) and electrochemical impedance spectroscopy (EIS) were performed using a Metrohm Autolab potentiostat/ galvanostat (PGSTAT 302 N). In EIS measurements, an ac potential of 10 mV amplitude was applied on the cell at a frequency range of $10^{-2} - 10^6$ Hz. For ex-situ XRD analyses, the coin cells undergo the first cycle, were charged and discharged to the respective potentials, then removed cathode, and carefully washed several times with propylene carbonate solvent. Finally, the cathodes were dried in a glove box filled with argon for 24 h before performing XRD measurements.

3. Results and discussion

Fig. 1 shows the X-ray diffraction pattern of the synthesized $Na_{1.0}Li_{0.2}Mn_{0.7}Ti_{0.1}O_2$ material. The sharp peaks can be indexed to a hexagonal P2-structure, space group of $P6_3/mmc$ without any impurity phase. In comparison with JCPDS No 27–0751, an additional "1/3 1/3 1" peak located at 2θ of 22.3° represents a long range in-plane ordering of Li and Mn ions [20]. All diffraction peaks are shifted toward higher 2θ angle suggesting a smaller distance between two adjacent MO_2 (M = Mn, Li, Ti) slabs, corresponded to a lower *c* value of lattice parameter of the $Na_{1.0}Li_{0.2}Mn_{0.7}Ti_{0.1}O_2$ material which compared to the JCPDS standard (*c* = 11.12 Å) [21]. Three single peaks located at the 2θ region of 60° to 70° are featured in the hexagonal P2-structure, unlike those of orthorhombic P2-structure which are splitting peaks [22]. The lattice parameters of the $Na_{1.0}Li_{0.2}Mn_{0.7}Ti_{0.1}O_2$ material were *a* = 2.8461 Å and *c* = 10.980 Å that were calculated by PowderCell software [48]. The smaller *c* value, compared to that of reported P2-structure materials [13,18,21], can be attributed to the lithium and titanium substituted for manganese which leaded to a decrease of repulsive force between two adjacent MO_2 slabs [23,24]. The hexagonal P2-structure of a typical Na_xMnO_2 material was illustrated in the inset of Fig. 1. The dark green balls, the red balls, and purple balls represented sodium ions, oxygen ions, and manganese ions, respectively. In the structure, the sodium ions located at two distinct prismatic sites (Na(f) and Na(e)), one is face-sharing and the other is edge-sharing with MnO_6 octahedral sites. In the charging process, the Na (f) ions will be extracted first because they are less electrostatic stable than the Na(e) ions [25].

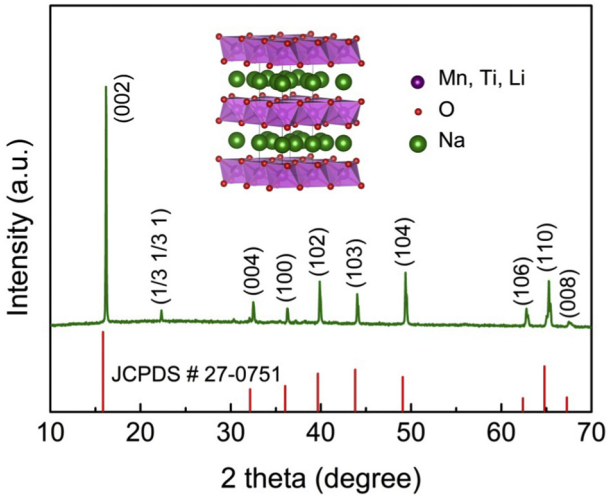

Fig. 1. X-ray diffraction pattern of $Na_{1.0}Li_{0.2}Mn_{0.7}Ti_{0.1}O_2$ material, and an illustration of a typical P2-type structure of Na_xMnO_2 material (inset).

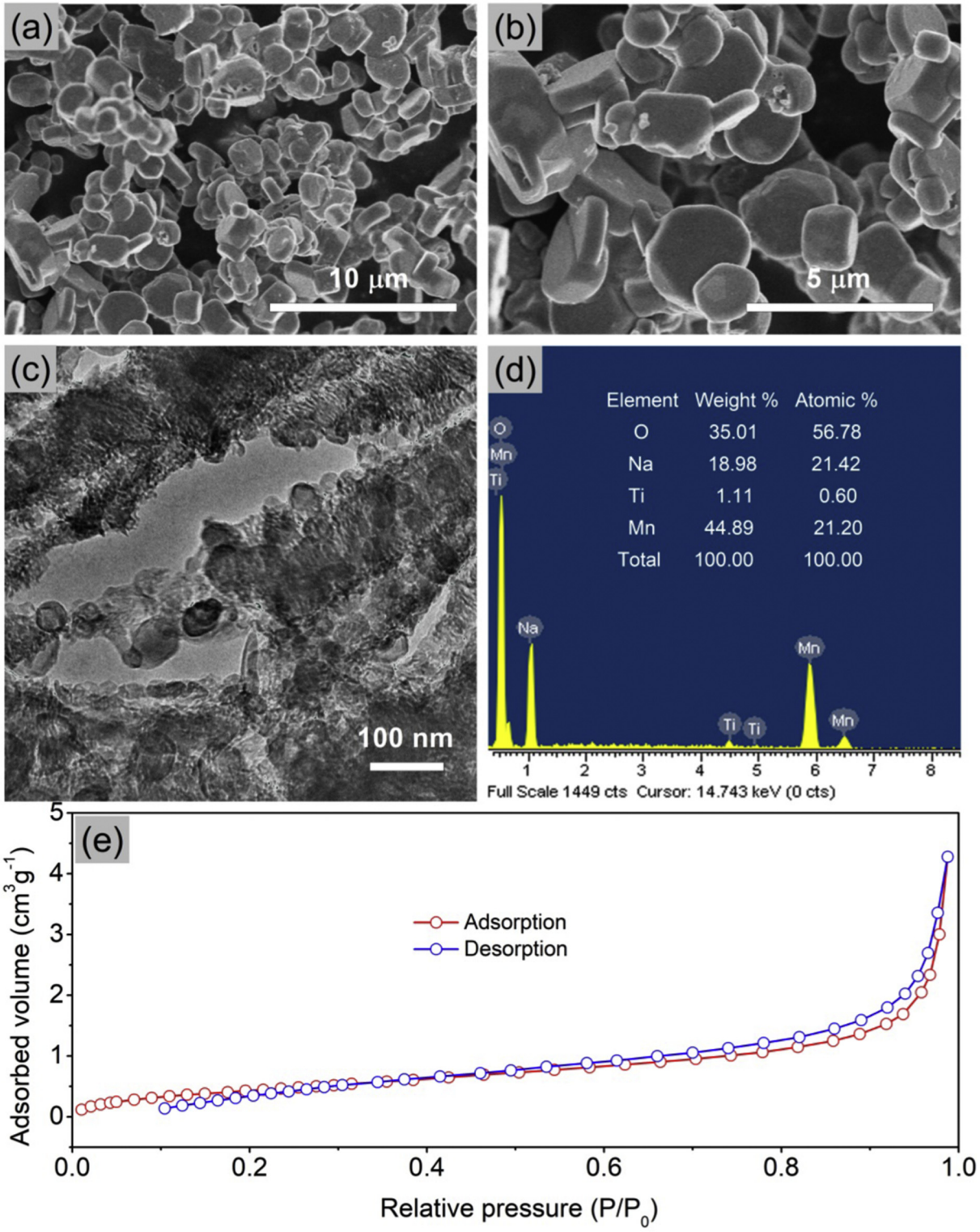

Fig. 2. SEM images (a, b), TEM image (c), the EDS analysis result (d), and nitrogen adsorption/desorption isotherms of $Na_{1.0}Li_{0.2}Mn_{0.7}Ti_{0.1}O_2$ material (e).

The SEM images of the $Na_{1.0}Li_{0.2}Mn_{0.7}Ti_{0.1}O_2$ material is shown in Fig. 2(a, b). The $Na_{1.0}Li_{0.2}Mn_{0.7}Ti_{0.1}O_2$ material has plate-like shape morphology with the main plate size of 1–3 μm. The morphology of the material is similar to that of a layered P2-$Na_{2/3}Co_{1/2}Ti_{1/2}O_2$ oxide, which was synthesized by the solid state reaction method at 900 °C for 12 h [18,25]. The fact that the P2-structured $Na_{1.0}Li_{0.2}Mn_{0.7}Ti_{0.1}O_2$ material was successfully synthesized at a low temperature (730 °C) revealed that the substitutions of lithium and titanium affected the crystallization of the material. It also should be note that many Na_xMO_2 materials contained titanium synthesized by solid state reaction method at a high temperature (900 °C) have different layered structure (O3-type) [28–30] and different morphologies such as spherical shape [31] and, layered morphology [32]. The capacities of the above-mentioned O3-structured materials are in the range of 90 mAh g^{-1} to 120 mAh g^{-1}. Fig. 2c shows TEM image of

$Na_{1.0}Li_{0.2}Mn_{0.7}Ti_{0.1}O_2$ material. As shown in the figure, the material is polycrystalline with many grains that are evenly distributed inside the $Na_{1.0}Li_{0.2}Mn_{0.7}Ti_{0.1}O_2$ particles. The EDX result (Fig. 2d) confirmed the presence of Na, Mn, Ti, O atomics in the $Na_{1.0}Li_{0.2}Mn_{0.7}Ti_{0.1}O_2$ material. The measured ratio between Na, Mn, Ti and O atomics is 0.754/0.747/0.02/2 which relatively closes to the stoichiometric ratio (1/0.7/0.1/2) of the formula $Na_{1.0}Li_{0.2}Mn_{0.7}Ti_{0.1}O_2$. The errors in the concentrations of Na and Ti can be explained by the low EDX sensitivity of Na and the insignificant concentration of Ti in the material.

The BET surface area analysis was performed for further investigation of the morphology of the synthesized material. The BET result of the material in Fig. 2e showed a type II isotherm which indicated non-porous morphology of the material [26]. The specific surface area of $Na_{1.0}Li_{0.2}Mn_{0.7}Ti_{0.1}O_2$ material that was calculated from the BET measurement is about 2 $m^2\ g^{-1}$. If the density of synthesized material is set equal to that of $Na_{0.7}MnO_2$ (4.21 g cm^{-3}) [27], the measured area will correspond to the surface area of 1 g of circular discs that have diameter and thickness of ca. 2 μm and 311 nm, respectively. These calculation results are in good agreement with those obtained from the SEM images.

The charge/discharge measurements were conducted within the potential range of 1.5 to 4 V at different rate from 0.1 to 1C, and the results were shown in Fig. 3. As shown in Fig. 3a, the discharge profiles of all three 1st, 5th, and 10th cycles were overlapping which suggested high stability of the $Na_{1.0}Li_{0.2}Mn_{0.7}Ti_{0.1}O_2$ structure. The 1st charge curve started at the open circuit voltage (OCV) of 3.1 V and showed a clear voltage plateau at 3.5 V. This voltage plateau also was observed on the 5th and the 10th cycle. The discharge curves showed only a corresponded clear voltage plateau at 2.7 V, unlike multiple voltage-plateau charge/discharge profiles of P2-$Na_{0.66}Ni_{0.25}Mn_{0.55}Ti_{0.2}O_2$ [6] and O3-$Na[Ti_x(Ni_{0.6}Co_{0.2}Mn_{0.2})_{1-x}]O_2$ materials [31]. The 1st, the 5th, and the 10th charge/discharge capacities of the $Na_{1.0}Li_{0.2}Mn_{0.7}Ti_{0.1}O_2$ material were 86/146 mAh g^{-1}, 159/149 mAh g^{-1}, and 156/148 mAh g^{-1}, respectively. The charge/discharge profiles and rate capability of the $Na_{1.0}Li_{0.2}Mn_{0.7}Ti_{0.1}O_2$ electrode at different current densities were shown in Fig. 3(b, c). All the charge/discharge curves were similar which revealed that the Na^+ ions extraction/insertion processes at different rates were reversible. The discharge capacities of the electrode at 0.1C, 0.2C, 0.5C, and 1.0C were 161, 138, 121, and 101 mAh g^{-1}, respectively. The phenomenon that the discharge capacity of the electrode returned to its initial value of 155 mAh g^{-1} (at 0.1C) after cycling at 1C rate confirmed the structural stability of the $Na_{1.0}Li_{0.2}Mn_{0.7}Ti_{0.1}O_2$ material at high rates of charge/discharge. Fig. 3d showed the cycling performance of the electrode when repeating charge/discharge measurement at a current density of 0.1C. The specific discharge capacity after 50 cycles was 134 mAh g^{-1}, corresponding to 90% of its initial value. This result provided evidence to prove the high reversibility of the electrochemical reaction occurring during charge/discharge. In addition, charge/discharge results also showed that the Coulombic efficiency of $Na_{1.0}Li_{0.2}Mn_{0.7}Ti_{0.1}O_2$ material increased during 10 initial cycles and after that, became stable at ca. 97%. This result suggested that the $Na_{1.0}Li_{0.2}Mn_{0.7}Ti_{0.1}O_2$ material seems to need several charge/discharge cycles to stabilize its structure.

It can be realized that the charge/discharge capacities of $Na_{1.0}Li_{0.2}Mn_{0.7}Ti_{0.1}O_2$ material in this study are higher than that of most related materials which were reported, such as P2-$Na_{0.7}MnO_2$ (101 mAh g^{-1} at 0.1C) [33], P2-$Na_{0.44}MnO_2$ (115 mAh g^{-1} at 0.1C) [34], P2-$Na_{0.80}$

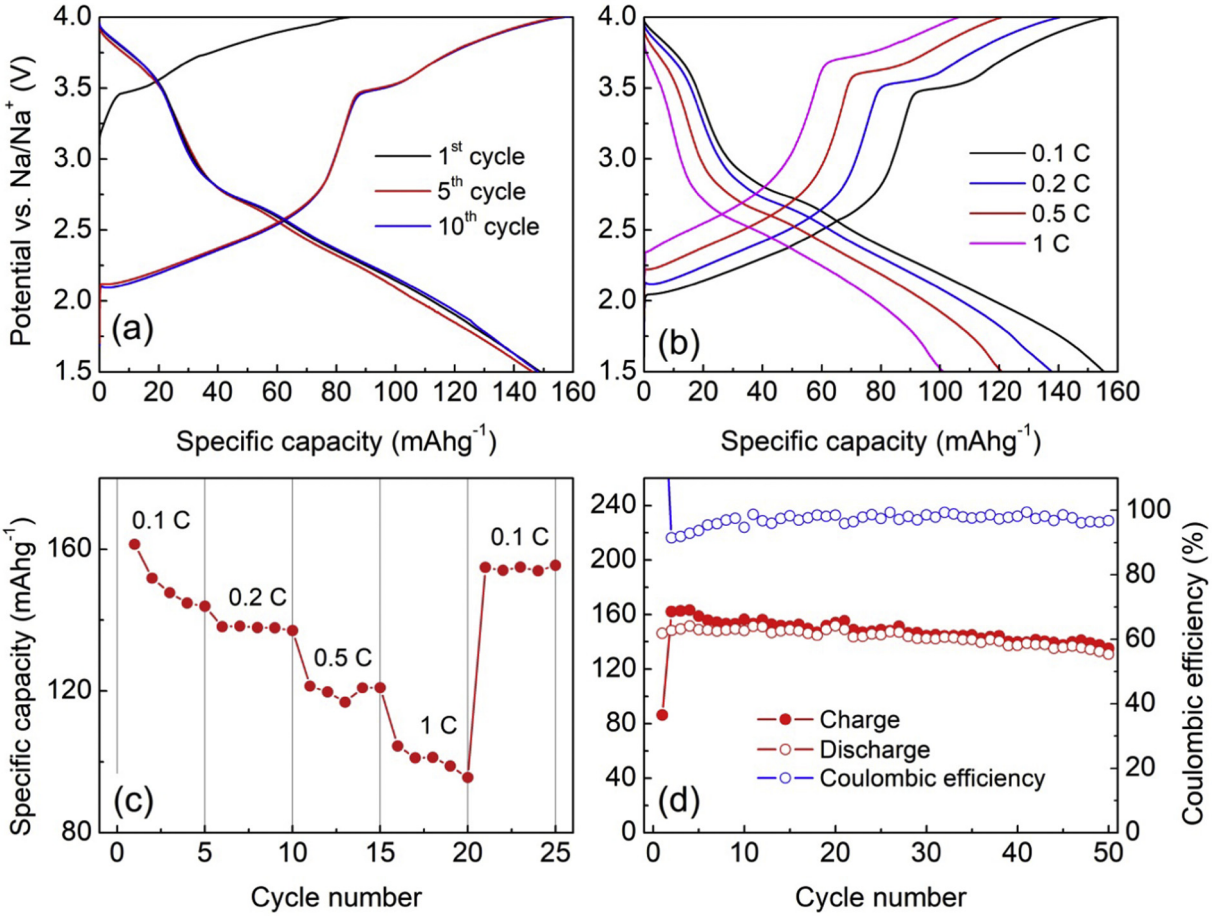

Fig. 3. The 1st, 5th, 10th charged/discharged profiles at 0.1C (a), charged/discharged curves at 0.1C, 0.2C, 0.5C and 1.0C (b), rate capability (c), and cycling ability (d) of the $Na_{1.0}Li_{0.2}Mn_{0.7}Ti_{0.1}O_2$ cathode in the potential range of 1.5–4 V vs Na/Na^+.

Table 1
Comparison of discharge capacity of P2-structure $Na_{1.0}Li_{0.2}Mn_{0.7}Ti_{0.1}O_2$ materials with that of previously reported P2-structure and O3-structure materials.

Electrode materials	Synthesized methods	Discharge capacities	References
P2-$Na_{0.7}MnO_2$	Solid-state reaction	101 mAh g^{-1} at 0.1C	[34]
P2-$Na_{0.44}MnO_2$	Solid-state reaction	115 mAh g^{-1} at 0.1C	[34]
P2-$Na_{0.80}[Li_{0.12}Ni_{0.22}Mn_{0.66}]O_2$	Solid-state reaction	120 mAh g^{-1} at 0.1C	[23]
P2-$Na_{0.44}[Mn_{0.78}Ti_{0.22}]O_2$	Solid-state reaction	110 mAh g^{-1} at 0.1C	[19]
P2-$Na_{0.7}Li_{0.3}Mn_{0.75}O_2$	Solid-state reaction	149 mAh g^{-1} at 0.1C	[36]
P2-$NaLi_{0.2}Mn_{0.8}O_2$	Solid-state reaction	241 mAh g^{-1} at 0.1C	[37]
P2-$Na_{0.6}[Cr_{0.6}Ti_{0.4}]O_2$	Solid-state reaction	75 mAh g^{-1} at 0.1C	[9]
P2-$Na_{2/3}Co_{1/2}Ti_{1/2}O_2$	Solid-state reaction	100 mAh g^{-1} at 0.1C	[25]
P2-$Na_{0.66}Ni_{0.25}Mn_{0.55}Ti_{0.2}O_2$	Solid-state reaction	114 mAh g^{-1} at 10 mA g^{-1}	[18]
P2-$Na_{0.85}Li_{0.17}Ni_{0.21}Mn_{0.64}O_2$	Solid-state reaction	100 mAh g^{-1} at 10 mA g^{-1}	[17]
P2-$Na_{0.80}[Li_{0.12}Ni_{0.22}Mn_{0.66}]O_2$	Solid-state reaction	120 mAh g^{-1} at 0.1C	[23]
$Na_{0.8}Li_{0.33}Mn_{0.62}Ti_{0.05}O_2$	Solid-state reaction	158 mAh g^{-1} at 0.1C	[38]
O3-$Na_{0.8}Ni_{0.35}Co_{0.1}Ti_{0.55}O_2$	Solid-state reaction	90 mAh g^{-1} at 0.1C	[29]
O3-$NaTi_{0.5}Ni_{0.5}O_2$	Solid-state reaction	121 mAh g^{-1} at 0.2C	[32]
O3-$Na_{0.8}Ni_{0.3}Co_{0.1}Ti_{0.6}O_2$	Solid-state reaction	88 mAh g^{-1} at 0.2C	[28]
P2-$Na_{1.0}Li_{0.2}Mn_{0.7}Ti_{0.1}O_2$	Solid-state reaction	160 mAh g^{-1} at 0.1C	This study

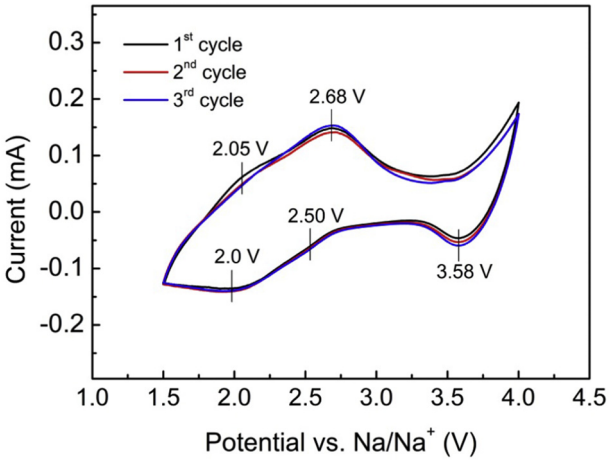

Fig. 4. The 1st, 2nd and 3rd CV curves of the $Na_{1.0}Li_{0.2}Mn_{0.7}Ti_{0.1}O_2$ electrode.

$[Li_{0.12}Ni_{0.22}Mn_{0.66}]O_2$ (120 mAh g^{-1} at 0.1C) [23], and P2-$Na_{0.44}[Mn_{0.78}Ti_{0.22}]O_2$ (110 mAh g^{-1} at 0.1C) [35]. In some other cases, P2-sodium-lithium-manganese oxides such as P2-$Na_{0.7}Li_{0.3}Mn_{0.75}O_2$ [36] and P2-$NaLi_{0.2}Mn_{0.8}O_2$ [37] exhibited comparable or higher capacities. However, these oxides presented low rate capability and poor cyclability. For further evaluation, a comparison of the discharge capacity of $Na_{1.0}Li_{0.2}Mn_{0.7}Ti_{0.1}O_2$ in this work with reported values of other P2-type and O3-type sodium manganese oxides is provided in Table 1.

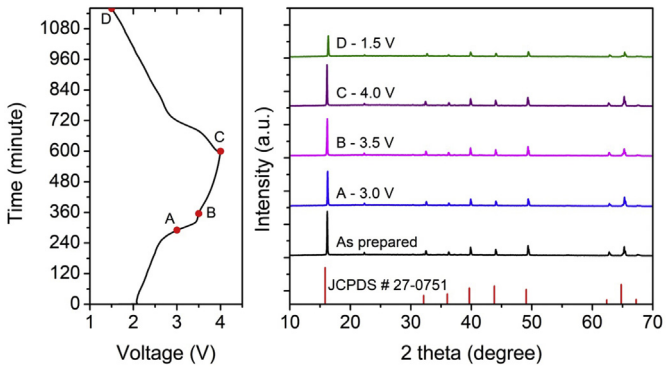

Fig. 5. Ex-situ XRD patterns of the $Na_{1.0}Li_{0.2}Mn_{0.7}Ti_{0.1}O_2$ material during charge/discharge process.

The higher performance of the $Na_{1.0}Li_{0.2}Mn_{0.7}Ti_{0.1}O_2$ material can be attributed to the higher sodium concentration and the existence of both lithium and titanium substituted for manganese in the MO_2 slab, which is preferable for more Na^+ ions insert/extract into/from the structure of the material [17,23]. The role of lithium in $Na_{1.0}Li_{0.2}Mn_{0.7}Ti_{0.1}O_2$ material in enhancing cycling performance has been proved by Meng et al. [23]. According to the authors, there are three main reasons that lead to the enhancement of electrochemical efficiency of $Na_{1.0}Li_{0.2}Mn_{0.7}Ti_{0.1}O_2$ material. First, the lithium ion prevents the phase transformation between P2 and O3 and subsequently to more stable P2-structure materials containing Li^+ compared to those without Li^+. Second, when Li^+ ions substitute the sites of P2-layered transition metal ions during charge process, they will migrate to the octahedral sites and are mostly recovered in the discharge process. Finally, Li^+ ions may lose a fraction in the first cycle, but they do not seem to be lost in the next cycles. Like the Li^+ ion, Ti^+ ions have also substituted the sites of transition Mn^{4+} randomly at octahedral sites [39]. Because the ionic size of Ti^{4+} (0.605 Å) is larger than Mn^{4+} (0.53 Å) [40], the distance between MO_6 (M = Li, Ti, Mn) layers increase and the Na^+ ions diffusion process occurs faster [41,42]. As a result, the electrochemical performance was enhanced.

The redox reactions of the $Na_{1.0}Li_{0.2}Mn_{0.7}Ti_{0.1}O_2$ material were characterized by cyclic voltammogram (CV) measurement at a potential range of 1.5–4.0 V with a scan rate of 0.2 mV s^{-1}. The CV profiles in Fig. 4 showed three anodic peaks at 2.05 V, 2.68 V, and 4.0 V on charge and three cathodic peaks at 2.0 V, 2.5 V, and 3.58 V on discharge. In fact, the oxidation/reduction processes in P2-type sodium manganese oxides are complex, with many anodic/cathodic peaks were observed on the CV and the dQ/dV profiles of the materials [33,43]. Recently, S. Komaba et al. assigned the first redox peaks at about 2–2.3 V to the first-order transition between P2 phases by using operando XRD measurements [44], but the origins of the other redox peaks are still not fully understood [45]. It is clear that fewer redox peaks are observed, fewer phase transitions occur in the material, however.

In order to evaluate structural stability of $Na_{1.0}Li_{0.2}Mn_{0.7}Ti_{0.1}O_2$ material, ex-situ XRD analysis was performed at different states of charge/discharge. Fig. 5 showed XRD patterns of $Na_{1.0}Li_{0.2}Mn_{0.7}Ti_{0.1}O_2$ cathode

Table 3
Lattice-parameter evolution of $Na_{1.0}Li_{0.2}Mn_{0.7}Ti_{0.1}O_2$ structure at different states of charge/discharge.

	a (Å)	*c* (Å)	Vol. (Å^3)
As prepared powder	2.8461	10.9800	77.02528
Charge to 3.0 V	2.8766	11.0844	79.43315
Charge to 3.5 V	2.8737	11.0893	79.30811
Charge to 4.0 V	2.8713	11.1066	79.29922
Discharge to 1.5 V	2.8844	11.0643	79.71967

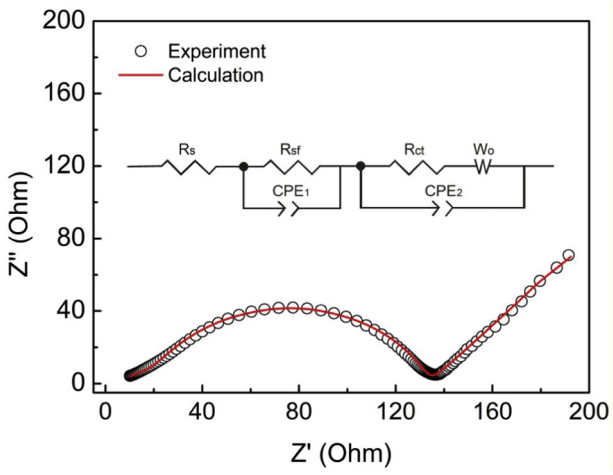

Fig. 6. Nyquist Plot and equivalent circuit (inset) that used to fit the EIS data of the as-prepared $Na_{1.0}Li_{0.2}Mn_{0.7}Ti_{0.1}O_2$ cell.

Table 2
Comparison of values of elements in the EIS equivalent circuit of different as-prepared cells.

Element	$NaLi_{0.2}Mn_{0.8}O_2$ [16]	$NaLi_{0.2}Mn_{0.6}Ni_{0.2}O_2$ [46]	$NaLi_{0.2}Mn_{0.6}Ti_{0.2}O_2$
R_s (Ω)	34.2	5	7.93
CPE_1 - T ($x10^{-5}$)	X	0.25	1.4
$CPE_1 - P$	X	0.875	0.68
R_{sf}	X	59	12
CPE_2 - T ($x10^{-4}$)	0.14	3.7	0.13
CPE_2 - P	0.718	0.86	0.79
R_{ct} (Ω)	376	334	113.6
Wo - R	3750	15,500	314.2
Wo - T	130	142	148
Wo - P	0.429	0.637	0.561

material as-prepared, charged to 3.0 V, charged to 3.5 V, charged to 4 V, and discharge to 1.5 V. Obviously, all of the states presented the same XRD patterns which was assigned to the P2-type layered structure. This result suggested that the structure of $Na_{1.0}Li_{0.2}Mn_{0.7}Ti_{0.1}O_2$ material was stable during charge/discharge. Based on the XRD patterns, the lattice parameters of $Na_{1.0}Li_{0.2}Mn_{0.7}Ti_{0.1}O_2$ at different states of charge/discharge were calculated and presented in Table 3. The calculated results showed that *a* constant increased while *c* constant decreased as the Na content in the material increased. This phenomenon may be explained by the increase of repulsive force between the MO_2 as a result of the extraction of Na^+ ions from the material [46]. The difference in unit-cell volumes at full charge (4 V) and full discharge (1.5 V) is only about 0.5%, indicating that the expansion/shrinkage of the P2-type structure of $Na_{1.0}Li_{0.2}Mn_{0.7}Ti_{0.1}O_2$ material is small during insertion and de-insertion of sodium ions. The unusually low values of the lattice constants of the pristine material may be attributed to the rearrangement of the atoms in the structure after the first cycle of charge/discharge. Also note that ex-situ XRD measurements were conducted on the electrodes, where the diffraction spectra of the active materials could be influenced by non-active materials such as black carbon and PVDF binder.

Fig. 6 showed Nyquist plots of the impedance data of as-prepared $Na_{1.0}Li_{0.2}Mn_{0.7}Ti_{0.1}O_2$ cell and the equivalent circuit that was used to fit the data. The Nyquist plot consists of a very small depressed semicircle at high frequency, an anomalous semicircle at intermediate frequency, and an inclined line at low frequency. In the equivalent circuit, the R_s element equals to value of ohmic resistance. The CPE_1 and R_{sf} elements, which correspond to the depressed semicircle, present a double layer and resistance at the surface of the electrode, respectively. The R_{ct} and CPE_2 elements, which represent to the anomalous semicircle, can be attributed to the charge-transfer resistance and the heterogeneity of the electrode surface, respectively [37,46]. The Nyquist plot of the $Na_{1.0}Li_{0.2}Mn_{0.7}Ti_{0.1}O_2$ material is similar to that of $Na_{1.0}Li_{0.2}Mn_{0.6}Ni_{0.2}O_2$ [46] and $Na_xMn_{1/2}Co_{1/2}O_2$ [47] materials. However, it is distinct from that of $Na_{1.0}Li_{0.2}Mn_{0.8}O_2$ material, which consists of only one semicircle and an inclined line [16].

The fitted values of the circuit elements were shown in Table 2. Due to same experimental conditions of the EIS measurements were also applied on the $Na_{1.0}Li_{0.2}Mn_{0.8}O_2$ and $Na_{1.0}Li_{0.2}Mn_{0.6}Ni_{0.2}O_2$ electrodes [16,46], the fitted values for these electrodes were also listed in the table for comparison. As seen in the table, the values of R_s, R_{ct} and Warburg impedance of the $NaLi_{0.2}Mn_{0.6}Ti_{0.2}O_2$ electrode were lower than those of the $Na_{1.0}Li_{0.2}Mn_{0.6}Ni_{0.2}O_2$ and $Na_{1.0}Li_{0.2}Mn_{0.7}Ti_{0.1}O_2$ electrodes. The decrease in the impedance values of the $Na_{1.0}Li_{0.2}Mn_{0.7}Ti_{0.1}O_2$ electrode once again revealed the advantages in the electrochemical performance of the synthesized material.

4. Conclusions

Single phase $Na_{1.0}Li_{0.2}Mn_{0.7}Ti_{0.1}O_2$ material with P2-type layered structure was successfully synthesized by the conventional solid-state reaction method. The electrochemical measurement results showed that the synthesized material exhibited greater capacitance, better cyclability, and higher rate capability than most of the other same type materials. The EIS and ex-situ XRD results revealed that the material had a good conductivity and a stable structure during charge/discharge. These advantages can be explained by synergistic effect of Li and Ti substitution at Mn sites in the structure of the synthesized material. Finally, the results of this study suggested that the $Na_{1.0}Li_{0.2}Mn_{0.7}Ti_{0.1}O_2$ material is a promising cathode for practical application in sodium ion batteries.

Author contributors

Nguyen V. To: Conceptualization, Data curation, Formal analysis, Investigation, Methodology, Supervision, Validation, Visualization, Writing - original draft, Writing - review & editing. Ky V. Nguyen: Data curation. Hieu S. Nguyen: Writing - review & editing. Son T. Luong: Visualization. Phat T. Doan: Visualization. Thu Hoa T. Nguyen: Data curation. Quyen Q. Ngo: Data curation, Formal analysis, Investigation, Methodology, Validation, Writing- review & editing. Nghia V. Nguyen: Conceptualization, Data curation, Formal analysis, Methodology, Project administration, Resources, Supervision, Visualization, Writing - original draft, Writing - review & editing.

Declaration of Competing Interest

None.

Acknowledgments

This research is funded by the Vietnam National Foundation for Science and Technology Development (NAFOSTED) under the grant number: 15/2020/TN.

References

[1] D. Carlier, et al., The P2-$Na_{2/3}Co_{2/3}Mn_{1/3}O_2$ phase: structure, physical properties and electrochemical behavior as positive electrode in sodium battery, Dalton Trans. 40 (36) (2011) 9306–9312.
[2] R.J. Clément, et al., Structurally stable Mg-doped P2-$Na_{2/3}Mn_{1-y}Mg_yO_2$ sodium-ion battery cathodes with high rate performance: insights from electrochemical, NMR and diffraction studies, Energy Environ. Sci. 9 (10) (2016) 3240–3251.
[3] K. Tang, et al., High-performance P2-type Fe/Mn-based oxide cathode materials for sodium-ion batteries, Electrochim. Acta 312 (2019).

[4] J. Li, et al., P2 – Type $Na_{0.67}Mn_{0.8}Cu_{0.1}Mg_{0.1}O_2$ as a new cathode material for sodium-ion batteries: Insights of the synergetic effects of multi-metal substitution and electrolyte optimization, J. Power Sources 416 (2019) 184–192.

[5] J.-Y. Li, et al., P2-type $Na_{0.53}MnO_2$ nanorods with superior rate capabilities as advanced cathode material for sodium ion batteries, Chem. Eng. J. (2017) 316.

[6] W.-L. Pang, et al., P2-type Na2/3Mn1/2Co1/3Cu1/6O2 as advanced cathode material for sodium-ion batteries: electrochemical properties and electrode kinetics, J. Alloys Compd. 790 (2019).

[7] W.-L. Pang, et al., P2-type Na 2/3 Mn 1-x Al x O 2 cathode material for sodium-ion batteries: Al-doped enhanced electrochemical properties and studies on the electrode kinetics, J. Power Sources 356 (2017) 80–88.

[8] T. Risthaus, et al., A high-capacity P2 Na2/3Ni1/3Mn2/3O2 cathode material for sodium ion batteries with oxygen activity, J. Power Sources 395 (2018) 16–24.

[9] Wang, Y., et al., P2-Na0.6[Cr0.6Ti0.4]O2 cation-disordered electrode for high-rate symmetric rechargeable sodium-ion batteries. Nat. Commun., 2015. 6: p. 6954.

[10] A. Caballero, et al., Synthesis and characterization of high-temperature hexagonal P2-Na0.6 MnO2 and its electrochemical behaviour as cathode in sodium cells, J. Mater. Chem. 12 (4) (2002) 1142–1147.

[11] N. Bucher, et al., Combustion-synthesized sodium manganese (cobalt) oxides as cathodes for sodium ion batteries, J. Solid State Electrochem. 17 (7) (2013) 1923–1929.

[12] N. Bucher, et al., Combustion-synthesized sodium manganese (cobalt) oxides as cathodes for sodium ion batteries, J. Solid State Electrochem. 17 (2013).

[13] N. Yabuuchi, et al., P2-type Na x [Fe 1/2 Mn 1/2]O 2 made from earth-abundant elements for rechargeable NaÂ batteries, Nat. Mater. 11 (2012) 512–517.

[14] W. Zhao, et al., Synthesis of metal ion substituted P2-Na2/3Ni1/3Mn2/3O2 cathode material with enhanced performance for Na ion batteries, Mater. Lett. 135 (2014) 131–134.

[15] K. Du, K.S. Ryu, G. Hu, Layered Lithium-sodium manganese oxide as a cathode material for Lithium ion batteries, ECS Electrochem. Lett. 2 (2013) A36–A38.

[16] V.-N. Nguyen, P.-W. Ou, I.M. Hung, Synthesis and electrochemical properties of sodium manganese-based oxide cathode material for sodium-ion batteries, Electrochim. Acta 161 (2015).

[17] D.-H. Kim, et al., Enabling sodium batteries using Lithium-substituted sodium layered transition metal oxide cathodes, Adv. Energy Mater. 1 (2011) 333–336.

[18] W. Zhao, et al., Enhanced electrochemical performance of Ti substituted P2-Na2/3Ni1/4Mn3/4O2 cathode material for sodium ion batteries, Electrochim. Acta 170 (2015).

[19] Y. Wang, et al., Ti-substituted tunnel-type Na0.44MnO2 oxide as a negative electrode for aqueous sodium-ion batteries, Nat. Commun. (2015) 6.

[20] N. Yabuuchi, et al., New O2/P2-type Li-excess layered manganese oxides as promising multi-functional electrode materials for rechargeable Li/Na batteries, Adv. Energy Mater. 4 (2014).

[21] J.-P. Parant, et al., Sur quelques nouvelles phases de formule NaxMnO2 (x≤1), J. Solid State Chem. 3 (1) (1971) 1–11.

[22] D. Su, et al., Single crystalline Na0.7MnO2 nanoplates as cathode materials for sodium-ion batteries with enhanced performance, Chemistry (Weinheim an der Bergstrasse, Germany) 19 (2013).

[23] J. Xu, et al., Identifying the critical role of Li substitution in P2-Na-x[LiyNizMn1-y-z]O-2 ($0 < x, y, z < 1$) intercalation cathode materials for high-energy Na-ion batteries, Chem. Mater. 26 (2014) 1260.

[24] J. Paulsen, J.R. Dahn, Studies of the layered manganese bronzes, Na2/3[Mn1 − xMx]O2 with M = Co, Ni, Li, and Li2/3[Mn1 − xMx]O2 prepared by ion-exchange, Solid State Ionics 126 (1999) 3–24.

[25] N. Sabi, et al., Layered P2-Na2/3Co1/2Ti1/2O2 as a high-performance cathode material for sodium-ion batteries, J. Power Sources 342 (2017) 998–1005.

[26] G. Fagerlund, Determination of specific surface by the BET method, Mater. Constr. 6 (1973) 239–245.

[27] Sébastien Patoux, Mickaël Dollé, Marca M. Doeff, Layered manganese oxide intergrowth electrodes for rechargeable lithium batteries. 2. substitution with Al, Chem. Mater. 17 (5) (2005) 1044–1054.

[28] S. Guo, et al., Cation-mixing stabilized layered oxide cathodes for sodium-ion batteries, Sci. Bull. 63 (2018).

[29] H. Guo, et al., Na-deficient O3-type cathode material Na0.8[Ni0.3Co0.2Ti0.5]O2 for roomerature sodium-ion batteries, Electrochim. Acta 158 (2015) 258–263.

[30] J. Wang, et al., High-rate performance O3-NaNi0.4Mn0.4Cu0.1Ti0.1O2 as a cathode for sodium ion batteries, J. Alloys Compd. (2019) 792.

[31] T.-Y. Yu, et al., High-performance Ti-doped O3-type Na[Ti x (Ni 0.6 Co 0.2 Mn 0.2) 1-x]O 2 cathodes for practical sodium-ion batteries, J. Power Sources 422 (2019) 1–8.

[32] H. Yu, et al., Novel titanium-based O3-type NaTi0.5Ni0.5O2 as a cathode material for sodium ion batteries, Chem. Commun. (Camb.) (2013) 50.

[33] M.A. Khan, et al., P2/O3 phase-integrated Na0.7MnO2 cathode materials for sodium-ion rechargeable batteries, J. Alloys Compd. 771 (2019) 987–993.

[34] K.-Y. Shen, et al., Spray pyrolysis and electrochemical performance of Na0.44MnO2 for sodium-ion battery cathodes, MRS Commun. (2017) 1–4.

[35] Y. Wang, et al., Ti-substituted tunnel-type Na0.44MnO2 oxide as a negative electrode for aqueous sodium-ion batteries, Nat. Commun. 6 (1) (2015) 6401.

[36] H. Yu, et al., Study on enhancing electrochemical properties of Li in layered compound Na0.7Li0.3Mn0.75O2, Electrochim. Acta 263 (2018) 474–479.

[37] N. Van Nghia, P.-W. Ou, I.M. Hung, Synthesis and electrochemical properties of sodium manganese-based oxide cathode material for sodium-ion batteries, Electrochim. Acta 161 (2015) 63–71.

[38] X.-H. Ma, et al., P2-type Na0.8(Li0.33Mn0.67-xTix)O2 doped by Ti as cathode materials for high performance sodium-ion batteries, J. Alloys Compd. 815 (2019) 152402.

[39] M.M. Doeff, T.J. Richardson, K.-T. Hwang, Electrochemical and structural characterization of titanium-substituted manganese oxides based on Na0.44MnO2, J. Power Sources 135 (1) (2004) 240–248.

[40] T.-Y. Yu, et al., High-performance Ti-doped O3-type Na[Tix(Ni0.6Co0.2Mn0.2)1-x]O2 cathodes for practical sodium-ion batteries, J. Power Sources 422 (2019) 1–8.

[41] S. Bao, et al., Improving the electrochemical performance of layered cathode oxide for sodium-ion batteries by optimizing the titanium content, J. Colloid Interface Sci. 544 (2019) 164–171.

[42] X.-H. Ma, et al., P2-type Na0.8(Li0.33Mn0.67-xTix)O2 doped by Ti as cathode materials for high performance sodium-ion batteries, J. Alloys Compd. 815 (2020) 152402.

[43] S. Kumakura, Y. Tahara, S. Sato, K. Kubota, S. Komaba, P′2-Na2/3Mn0.9Me0.1O2 (Me = Mg, Ti, Co, Ni, Cu, and Zn): correlation between orthorhombic distortion and electrochemical property, Chem. Mater. 29 (2017) 8958–8962.

[44] S. Kumakura, Y. Tahara, K. Kubota, K. Chihara, S. Komaba, Sodium and manganese stoichiometry of P2-type Na2/3MnO2, Angew. Chem. Int. Ed. 55 (2016) 1–5.

[45] K. Kubota, S. Kumakura, Y. Yoda, K. Kuroki, S. Komaba, Electrochemistry and solid-state chemistry of NaMeO2 (Me = 3d transition metals), Adv. Energy Mater. 8 (2018) 1703415.

[46] V.-N. Nguyen, P.-W. Ou, I.M. Hung, Synthesis and Electrochemical Performances of layered NaLi0.2Ni0.2Mn0.6O2 cathode for sodium-ion batteries, Ceram. Int. (2015) 41.

[47] X. Wang, et al., Electrode properties of P2–Na2/3MnyCo1–yO2 as cathode materials for sodium-ion batteries, J. Phys. Chem. C 117 (30) (2013) 15545–15551.

[48] W. Kraus, G. Nolze, POWDER CELL - a program for the representation and manipulation of crystal structures and calculation of the resulting X-ray powder patterns, J. Appl. Crystallogr. 29 (1996) 301–303.